Functional Interactions Between A' Helices in the C-linker of Open CNG Channels

Li Hua and Sharona E. Gordon

Department of Physiology and Biophysics, University of Washington, Seattle, WA 98195

ABSTRACT Cyclic nucleotide-gated (CNG) channels are nonselective cation channels that are activated by the direct binding of the cyclic nucleotides cAMP and cGMP. The region linking the last membrane-spanning region (S6) to the cyclic nucleotide binding domain in the COOH terminus, termed the C-linker, has been shown to play an important role in coupling cyclic nucleotide binding to opening of the pore. In this study, we explored the intersubunit proximity between the A' helices of the C-linker regions of CNGA1 in functional channels using site-specific cysteine substitution. We found that intersubunit disulfide bonds can be formed between the A' helices in open channels, and that inducing disulfide bonds in most of the studied constructs resulted in potentiation of channel activation. This suggests that the A' helices of the C-linker regions are in close proximity when the channel is in the open state. Our finding is not compatible with a homology model of the CNGA1 C-linker made from the recently published X-ray crystallographic structure of the hyperpolarization-activated, cyclic nucleotide-modulated (HCN) channel COOH terminus, and leads us to suggest that the C-linker region depicted in the crystal structure may represent the structure of the closed state. The opening conformational change would then involve a movement of the A' helices from a position parallel to the axis of the membrane to one perpendicular to the axis of the membrane.

KEY WORDS: CNG channel • gating • oxidation • structure • cGMP

INTRODUCTION

Cyclic nucleotide-gated (CNG) channels are nonselective cation channels that transduce sensory stimuli into electrical signals in visual and olfactory receptor cells (Kaupp et al., 1989). Six different genes encode CNG channels, four A subunits (A1 to A4) and two B subunits (B1 and B3) (Richards and Gordon, 2000; Kaupp and Seifert, 2002). CNG channels function as homotetramers and heterotetramers in exogenous expression systems, but appear to be exclusively heterotetramers in vivo (Kaupp and Seifert, 2002). They share the same membrane topology as voltage-gated channels, with six transmembrane segments, intracellular NH_2 and COOH termini, and sequence similarity in the pore-lining region (Jan and Jan, 1990, 1992). However, CNG channels are activated by the direct binding of the cyclic nucleotides cAMP and cGMP to a cyclic nucleotide-binding domain in the COOH-terminal region of each subunit, and not by voltage.

Although both the cyclic nucleotide-binding domain and the ion-conducting pore in CNG channels have been structurally defined, based on their homology to ion channels whose structural elements have been solved, the mechanism by which the energy provided by cyclic nucleotide binding is converted into opening of the pore is not understood. A region linking the last membrane-spanning region (S6) to the cyclic nucleotide binding domain in the COOH terminus (the C-linker) has been shown to play an important role in channel gating. Previous experiments suggest that the C-linker controls coupling of ligand binding to channel gating, and that the movement of this region is closely coupled to channel activation (Gordon and Zagotta, 1995a,c; Tibbs et al., 1997; Paoletti et al., 1999; Johnson and Zagotta, 2001).

Divalent transitional metal (Ni^{2+}) binding to the C-linker of CNG channels has been used to demonstrate that open-state specific intersubunit interactions occur between proximal C-linker regions (Gordon and Zagotta, 1995a,b; Johnson and Zagotta, 2001). Given that amino acids coordinating Ni^{2+} must be within ~4 Å of each other (Maroney, 1999), these experiments strongly suggest that at least part of the proximal C-linker region must be a site for intersubunit proximity. Furthermore, at several sites, Ni^{2+} coordination occurs preferentially in the open state, providing a constraint on the proximity of this region in the open state. A later study using a histidine scan of the proximal C-linker of CNGA1 reported that stripes of sites separated by 50 degrees on an α-helix produced Ni^{2+} potentiation or Ni^{2+} inhibition

Correspondence to Sharona E. Gordon: seg@u.washington.edu

The online version of this article contains supplemental material.

Abbreviations used in this paper: CNBD, cyclic nucleotide-binding domain; CNG, cyclic nucleotide-gated; DTT, dithiothereitol; HCN, hyperpolarization-activated, cyclic nucleotide-modulated.

J. Gen. Physiol. © The Rockefeller University Press • 0022-1295/2005/03/335/10 $8.00
Volume 125 March 2005 335–344
http://www.jgp.org/cgi/doi/10.1085/jgp.200409187

(Johnson and Zagotta, 2001). These results suggest that the C-linker region undergoes a rotational movement during channel activation. This rotation may initiate movement of S6 and pore opening.

Hyperpolarization-activated, cyclic nucleotide-modulated channels (HCN) contain a C-linker region that is closely related to CNGA1 based on sequence similarity. The sequences of HCN2 and CNGA1 in the C-linker are 22% identical and 45% conserved overall (Fig. 1 A). Recently, a crystal structure of the COOH-terminal region of the HCN2 channel was solved to 2.0 Å resolution (Zagotta et al., 2003). This structure includes the C-linker and the cyclic nucleotide-binding domain (CNBD) bound to cAMP. In this structure, four HCN2 COOH termini are associated to form a tetramer. The C-linker region consists of six α-helices, designated A' to F', which are separated by short loops (Fig. 1 A). The C-linker regions also form a large interface of subunit–subunit interaction with 2,300 Å^2 of buried solvent-accessible surface area. In contrast, the CNBD regions show very little intersubunit contact. This structure suggests that the C-linker regions mediate the primary intersubunit interactions of the COOH termini of HCN2. Based on the high sequence similarity between the COOH termini of HCN2 and CNGA1 (Fig. 1 A), the CNGA1 C-linker regions may have similar structural and functional importance.

We constructed a model of the CNGA1 C-linker by threading the sequence of CNGA1 through the structure of HCN2 (Fig. 1 B). In this model, four CNGA1 C-linkers are associated to form a tetramer. Surprisingly, the structural relationships between C-linker regions in this model are not compatible with previous experiments on functional channels. For example, in this model, the distances between 420H residues in adjacent and opposite subunits are 35.12 Å and 50.18 Å, respectively. These distances are too large to allow high-affinity Ni^{2+} coordination, and raise the question of whether our homology model represents a meaningful structure of the CNG channel C-linker under physiological conditions.

In this study, we explored the intersubunit proximity between the C-linker regions of CNGA1 in functional channels using a site-specific cysteine substitution method (Falke et al., 1988). We found that intersubunit disulfide bonds can be formed between the A' helices of the C-linker regions during channel activation, indicating that these regions are in close proximity. Under our experimental conditions, most of the intersubunit disulfide bonds in this region potentiated channel activation, reflected as an increased apparent affinity for cGMP. We mapped the residues that formed intersubunit disulfide bonds onto a homology model of CNGA1, based on the structure of HCN2. Our data are not compatible with a model in which the C-linker conformation represents that of the open state, and suggest that the conformation seen in the structure may in fact represent the closed state.

MATERIALS AND METHODS

Site-directed Mutagenesis

We introduced individual cysteines into the amino acid positions from 417 to 424 in a cysteineless background CNGA1 channel (Matulef et al., 1999) in the pGEMHE vector according to previously published methods (Rosenbaum et al., 2004). In brief, fragments of cDNA were amplified in PCR using oligonucleotides synthesized to contain a cysteine mutation in combination with other wild-type oligonucleotides. The cDNA fragments were then cut with two different restriction enzymes to generate a cassette containing the mutation. The cassette was then ligated into the cysteineless CNGA1 cut with the same two restriction enzymes. After transformation of bacteria with the ligation product, single positive colonies were selected, and the entire region of the amplified cassette was sequenced to check for the mutation and ensure no second-site mutations. cDNAs of the new constructs were linearized with NheI and transcribed in vitro, using the T7 mMessage mMachine kit (Ambion). For all the mutants, the native histidine at the 420 amino acid position was mutated to glutamine to eliminate the potential modification of 420H in our oxidation experiments (Gordon and Zagotta, 1995a). Throughout the text, $CNGA1_{cysless}$ refers to the cysteineless background CNGA1 channel, and other cysteine mutants are named by the position of the mutated amino acid followed with "C," for example, 417C and 418C.

Heterologous Expression of Channels in Xenopus Oocytes

Segments of ovary were removed from anesthetized *Xenopus laevis*. After gross mechanical isolation, oocytes were isolated by agitating the sections of ovary in a Ca^{2+}-free collagenase (2.3 mg/ml) solution for up to 1.5 h. The cells were then rinsed and stored in frog Ringers solution at 14°C. Oocytes were generally injected with 40 nl cRNA solutions (~1 μg/μl) within 2 d of harvest. Electrophysiological recordings were performed 2–10 d after injection.

Electrophysiology

Inside-out membrane patches were obtained by using fire polished borosilicate pipettes (1.5 mM OD, 1.2 mM ID; Sutter Instrument Co.). Recordings were made using symmetrical NaCl/HEPES/EDTA solutions consisting of 130 mM NaCl, 3 mM HEPES, 0.2 mM EDTA (pH 7.2) with cGMP or cAMP added to the intracellular solution only. Copper (II) phenanthroline (Cu/P) (Kobashi, 1968) was prepared as follows: a 5 mM 1,10-phenanthroline stock in dry ethanol and a 1.5 mM cupric sulfate stock in water were diluted to final concentrations of 5 μM phenanthroline and 1.5 μM cupric sulfate in a solution containing 130 mM NaCl and 3 mM HEPES (pH 7.2); 2 mM cGMP or 128 μM cGMP (as indicated in the text) were present in this solution as well. Cu/P solutions were used for up to 2 d after preparation. Cu/P was applied to the intracellular side of patches for 3–10 min, as indicated in the text and figure legends. Dithiothereitol (DTT) was made as a 1 M stock in the NaCl/HEPES/EDTA solution and diluted to a final concentration of 5 mM in the NaCl/HEPES/EDTA solution together with 64 μM cGMP. The DTT solution was made fresh daily.

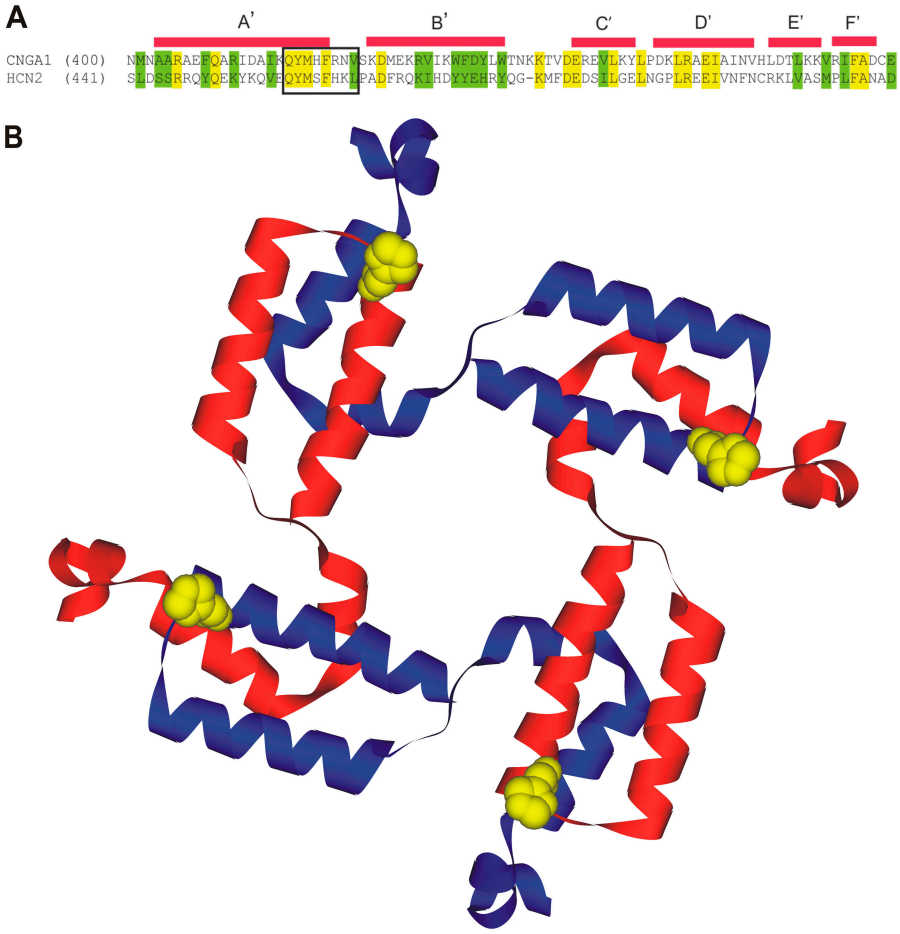

FIGURE 1. Sequence alignment of the C-linker regions between CNGA1 and HCN2 and structural model of the C-linker regions of CNGA1. (A) Sequence alignment of the C-linker regions between CNGA1 and HCN2. Green indicates conserved sequence and yellow indicates identical sequence. The square indicates the cysteine mutation region. (B) Structural model of CNGA1 C-linker based on the crystal structure of HCN2 channel COOH termini, with red and blue used to show alternate subunits. The model was built using the software Swiss-PDB viewer in conjunction with the Swiss-Model protein modeling server (Guex and Peitsch, 1997). The yellow residues indicate 420H in each subunit. The distance between 420H is 35.12 Å for adjacent subunits, and 50.18 Å for opposite subunits.

For macroscopic current measurements, pipettes were polished to a resistance between 0.3 and 1 MΩ. Currents were low-pass filtered at 2 kHz and sampled at 10 kHz with an Axopatch 200B (Axon Instruments, Inc.). All recordings were made at room temperature. Data were acquired and analyzed with PULSE data acquisition software (Heka Elektronik) and were plotted and fitted using Igor Pro (Wavemetrics Inc.). All currents shown have had currents in the absence of cyclic nucleotide subtracted. All currents were measured at +100 mV. For each experiment, currents at different cGMP concentrations were measured, and we waited until the currents had stabilized before proceeding. This delay was necessary because of the "run-up" caused by dephosphorylation of the channel by endogenous patch-associated phosphatases (Gordon et al., 1992; Molokanova et al., 1997). Smooth curves shown in dose–response relations are fits of the data to the Hill equation: $I = I_{max}([cGMP]^n/(K_{1/2}{}^n + [cGMP]^n))$. Data are reported as the mean ± SEM. Statistical significance was assayed with two-tailed Student's *t* tests.

For single channel recordings, pipettes were polished to a resistance between 8 and 12 MΩ. Currents were low-pass filtered at 5 kHz (eight-pole Bessel) and sampled at 10 kHz with an EPC10 amplifier (Heka Elektronik). Patches were held at 0 mV and stepped to +50 mV for 1 s. The presence of single channels in the patches was confirmed by application of 2 mM cGMP. Open probability (P_o) was calculated from fits to the data with two Gaussians. The area under the curve representing open channels relative to the total area was taken as P_o. Cu/P was applied to the intracellular side of the patches for 10 min for all single-channel experiments. Other solutions and software for data acquisition and analysis were the same as for the macroscopic current measurements.

Online Supplemental Material

Fig. S1 shows that Ni^{2+} both potentiates and inhibits 417H. cGMP dose–response curves without Ni^{2+} (open circles) and with 1 μM Ni^{2+} (filled circles). The smooth curves represent fits with the Hill equation with $K_{1/2}$ = 32.3 μM, Hill slope = 1.9 initially, and $K_{1/2}$ = 22 μM, Hill slope = 1.1 with 1 μM Ni^{2+}. The mean $K_{1/2}$ for activation by cGMP decreased from 32 ± 5.7 μM in the absence of Ni^{2+} to 17.4 ± 3.5 μM in the presence of Ni^{2+} (n = 3). The supplemental material is available at http://www.jgp.org/cgi/content/full/jgp.200409187/DC1.

RESULTS

Cu/P Induced Potentiation in Three of the Seven Cysteine Mutants in the A' Helix of the C-linker Region

We used disulfide bond formation between cysteine residues as a reporter of proximity between subunits. We introduced individual cysteines into different amino acid positions in the A' helix of the C-linker region of CNGA1 in the context of a cysteineless background ($CNGA1_{cysless}$). Copper (II) phenanthroline (Cu/P) oxidation was used to promote disulfide bond formation. Using disulfide bonds as indicators of proximity has

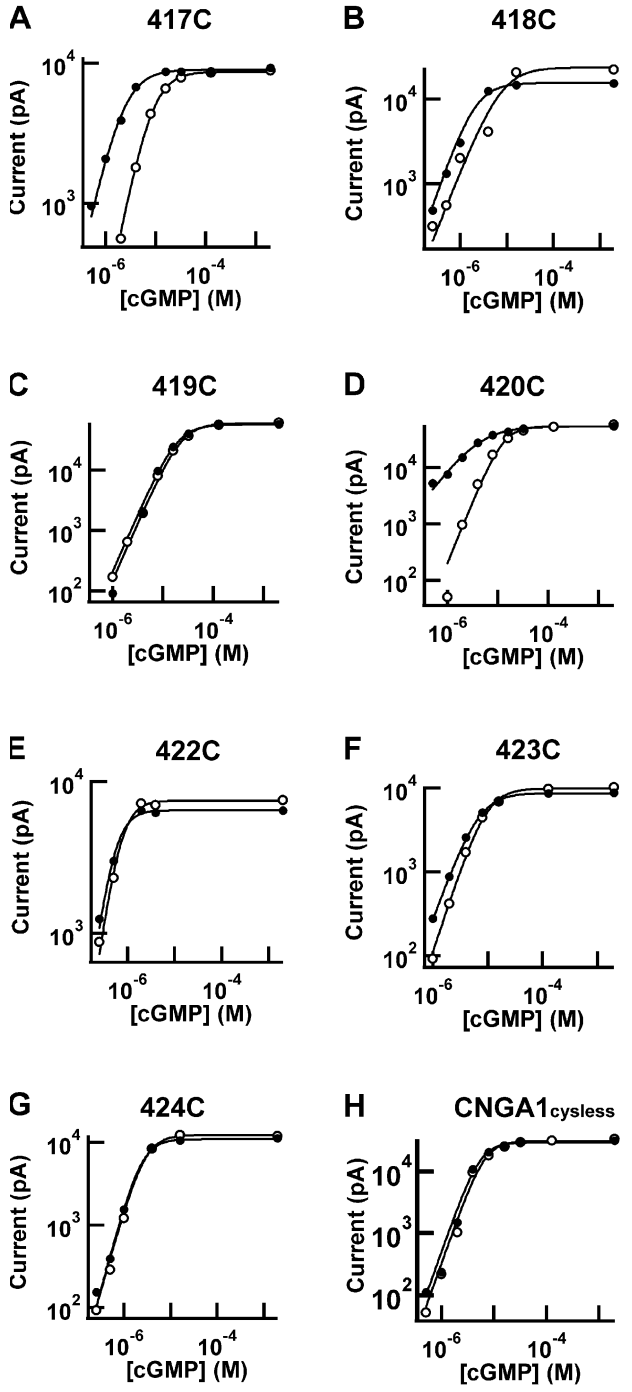

FIGURE 2. Cu/P induced potentiation in three of the seven cysteine mutants. Dose–response curves of cysteine mutants and $CNGA1_{cysless}$ activated by cGMP initially (open circles) and after (filled circles) treatment with Cu/P plus 2 mM cGMP. Smooth curves represent fits with the Hill equation (see MATERIALS AND METHODS), with mean $K_{1/2}$ values listed in Table I.

several advantages. For our mutant channels, which contain only one cysteine in each subunit, a disulfide bond can only be formed between cysteines from two different subunits; there is no ambiguity about whether the proximity is between two subunits or within a subunit. In addition, for a disulfide bond to form, the α carbons of the two cysteines must be within ~7 Å of each other (Falke et al., 1988). This distance is much shorter than the distance between 420H in our homology model (Fig. 1 B), and provides an important test of this model.

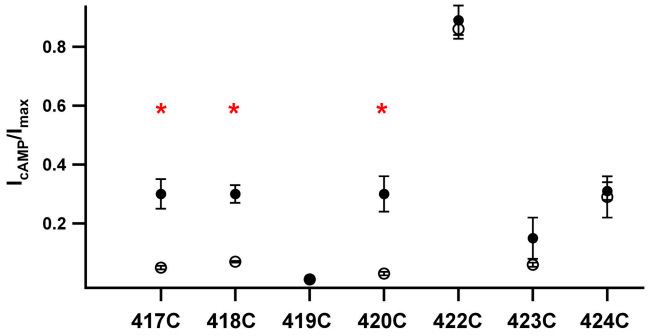

FIGURE 3. Cu/P effect on the current activated by saturating cAMP. Fraction of the current activated by 20 mM cAMP versus 2 mM cGMP (IcAMP/Imax) initially (open circles) and after Cu/P treatment (filled circles). Points represent the mean, with error bars representing the SEM. Patch numbers range from 4 to 8. Red * denotes a statistical difference of $P < 0.01$ (Student's t test) between the initial data and that after Cu/P treatment.

We substituted a cysteine for each of the amino acids from 417 to 424 individually in the $CNGA1_{cysless}$ (Matulef et al., 1999) background. All the mutants were functional except 421C. Mutant channels were expressed in *Xenopus* oocytes and examined using the inside-out configuration of the patch-clamp technique. To ensure that introduction of each cysteine did not prevent formation of functional, cyclic nucleotide-activated channels, we first measured the dose–response relation for activation of the mutant channels by cGMP (Fig. 2, open circles) and calculated the $K_{1/2}$ (Table I, $K_{1/2}$ initial; see MATERIALS AND METHODS), and also measured the fractional activation by a saturating concentration of the partial agonist cAMP (Fig. 3, open circles). We next used Cu/P to induce disulfide bond formation in each of the cysteine mutants. Two general types of outcomes are possible. If the regions containing the cysteines move during gating, then a disulfide bond that locks two of these regions together would be expected to perturb gating. If relative movement of the region containing the cysteines does not occur as part of gating, then locking the regions together through disulfide bond formation is not expected to perturb function. A third possibility, that no disulfide bond forms, cannot be functionally distinguished from a scenario in which a disulfide bond forms but does not alter channel properties.

After incubating the patches in Cu/P with 2 mM cGMP for 3–10 min, we remeasured the cGMP dose–response curve (Fig. 2, filled circles) and fractional activation by cAMP (Fig. 3, filled circles). For mutants

TABLE I

Apparent Affinity for cGMP Before and After Cu/P Treatment

Construct	$CNGA1_{cysless}$	417C	418C	419C	420C	422C	423C	424C
$K_{1/2}$, initial (μM)	9.49 ± 0.747 ($n = 6$)	7.61 ± 0.343 ($n = 5$)	6.19 ± 0.497 ($n = 8$)	26.45 ± 4.962 ($n = 4$)	16.73 ± 2.542 ($n = 9$)	0.82 ± 0.081 ($n = 12$)	5.56 ± 0.408 ($n = 12$)	3.81 ± 0.870 ($n = 7$)
$K_{1/2}$, after Cu/P (μM)	7.84 ± 1.510 ($n = 4$)	2.50 ± 0.333[a] ($n = 5$)	3.37 ± 0.506[a] ($n = 4$)	22.85 ± 0.917 ($n = 4$)	3.05 ± 0.873[a] ($n = 8$)	0.83 ± 0.147 ($n = 4$)	3.95 ± 0.890 ($n = 5$)	3.21 ± 0.830 ($n = 4$)

Properties of cysteine mutants compared to $CNGA1_{cysless}$ channel. For each construct, cGMP dose–response curves were measured before and after Cu/P application, and data are fitted with Hill equation. $K_{1/2}$ before and after Cu/P application was calculated and compared using Student's *t* test.
[a]$P < 0.01$.

419C, 422C, 423C, 424C, and the cysteineless channel $CNGA1_{cysless}$, Cu/P did not cause a significant change in the cGMP dose–response curve (Fig. 2, filled circles) or of the fractional activation by cAMP (Fig. 3, filled circles). In contrast, for 417C, 418C, and 420C Cu/P significantly shifted the cGMP dose–response curve to the left (Fig. 2), causing a decrease in $K_{1/2}$ (Table I). For these three cysteine mutants, the fractional activation by cAMP was also significantly increased (Fig. 3, filled circles). Although decreases in $K_{1/2}$ could arise from either a potentiation of gating or an increased affinity for binding cGMP, the increase in maximal activation by the partial agonist cAMP can arise only from potentiation of gating. Thus, Cu/P produced potentiation of gating in 417C, 418C, and 420C. Interestingly, for mutant 418C, Cu/P also decreased the maximal cGMP activated current (Fig. 2 B), a phenomenon we will discuss later.

Cu/P Effect Can Be Reversed by DTT

Under our oxidation conditions, Cu/P is expected to induce formation of a disulfide bond between cysteines from two subunits. However, it is possible that Cu/P would overoxidize the cysteines into sulfinic, sulfenic, or sulfonic acid (Torchinskii, 1974). One way to differentiate between such overoxidation and disulfide bond formation is to use the reducing agent DTT, which will reduce disulfide bonds but not overoxidized cysteines (Torchinskii, 1974). Fig. 4 shows examples of experiments with 417C, in which DTT was applied after Cu/P treatment. For 417C, the cGMP dose–response curve was measured initially, after Cu/P treatment, and after DTT treatment (Fig. 4 A, open, black, and red, respectively). Cu/P potentiated 417C function, shifting the cGMP dose–response curve to the left. Subsequent application of 5 mM DTT for 10 min to the intracellular side of the patch substantially reversed the Cu/P effect, shifting the dose–response relation for activation by cGMP back to the right.

We also measured the time course of disulfide bond reduction by DTT. An example of the time course is shown in Fig. 4 B. For these experiments, we measured a saturating concentration of cGMP (2 mM) as well as a subsaturating concentration (either 1 or 2 μM). As described above, Cu/P produced a large increase in the current activated by the subsaturating concentration of cGMP (Fig. 2 B, filled circles). Treatment with 5 mM DTT reversed this potentiation. For four patches exam-

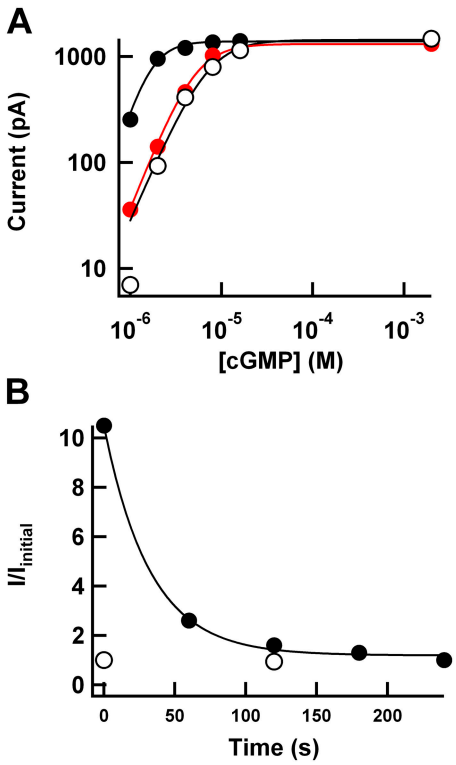

FIGURE 4. DTT reversed the effect of Cu/P treatment. (A) DTT reversed Cu/P potentiation of 417C. cGMP dose–response curves initially (open circles), after a 5-min treatment with Cu/P plus 128 μM cGMP (black circles), and after treatment with 5 mM DTT + 64 μM cGMP for 10 min (red circles). The smooth curves are fits with the Hill equation, with the following parameters: initially $K_{1/2}$ = 7.04 μM, Hill slope = 2.0 (black curve, right), after Cu/P $K_{1/2}$ = 1.61 μM, Hill slope = 2.8 (black curve, left), after DTT $K_{1/2}$ = 5.03 μM, Hill slope = 2.2 (red curve). (B) Time course of DTT reversing the potentiation effect of Cu/P on 417C. Normalized currents activated by 2 μM cGMP (black circles) and 2 mM cGMP (open circles) at +100 mV after a 5-min treatment with Cu/P plus 128 μM cGMP, and then various cumulative time in 5 mM DTT plus 64 μM cGMP. Smooth curve represents single exponential fit of the data, with time constant = 37.0 s.

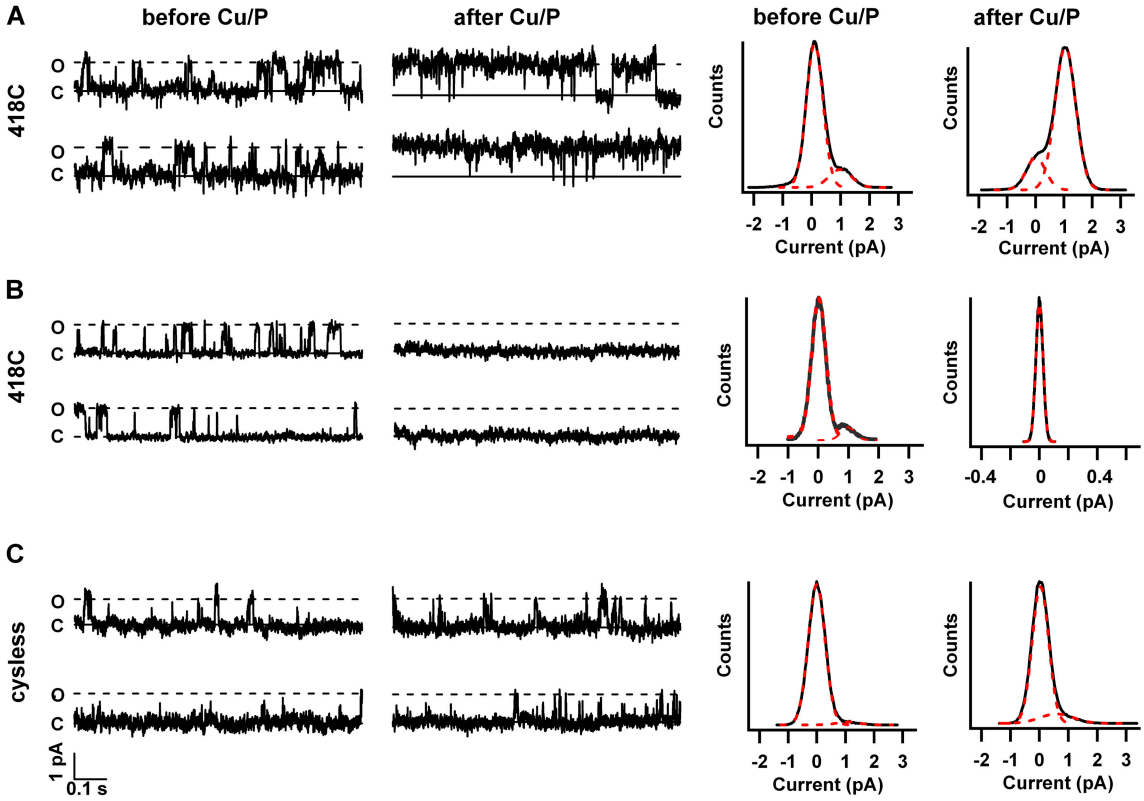

FIGURE 5. Cu/P produced two populations of channels in 418C. Single channel currents measured at +50 mV were recorded before and after a 10-min treatment with Cu/P plus 2 mM cGMP for 418C (A and B) and CNGA1$_{cysless}$ channels (C). For 418C, 4 μM cGMP was used to activate the channels, and for CNGA1$_{cysless}$, 2 μM cGMP was used to activate the channels. All-points histograms were made from the data collected under each condition (right, in all cases >5 s of data was used).

ined, the mean time constant for reversal was 37.3 s (± 6.0 s), and the ratio of the current after recovery to the initial current (ratio of the current at t = 180s to the initial current) was 1.1 (±0.12). These experiments indicate that Cu/P perturbed channel function by inducing formation of disulfide bonds between cysteines from different subunits. Our experiments therefore suggest that the A' helices of the C-linker region must be in very close proximity. Furthermore, the shift in the $K_{1/2}$ toward lower cGMP concentrations and the increased fractional activation by cAMP indicate that disulfide bond formation stabilized the open state of the channels relative to the closed state. The simplest interpretation of this potentiation of gating is that the intersubunit proximity caught by disulfide bond formation reflects open state proximity.

Potentiation and Inhibition by Cu/P

We next asked whether the combination of potentiation and inhibition observed at position 418 was an artifact of disulfide bond formation. We wondered if a mixture of potentiation and inhibition could be observed with Ni^{2+} as well. When we applied 1 μM Ni^{2+} to 417H channels, we observed both a reduction in the current activated by high concentrations of cGMP and an increase in the current activated by quite low concentrations of cGMP (Fig. S1, available at http://www.jgp.org/cgi/content/full/jgp.200409187/DC1), in contrast to previous reports (Gordon and Zagotta, 1995b; Johnson and Zagotta, 2001). This finding suggests that the dual effect of potentiation and inhibition is not unique to Cu/P modulation, but can be observed with Ni^{2+} binding as well.

In our experiments, Cu/P treatment of 418C potentiated gating, as measured by low concentrations of cGMP and by the fractional activation by cAMP, but also decreased the maximal current activated by cGMP. Does disulfide bond formation at 418C produce potentiation or inhibition? This is an important point, because we interpret potentiation as open-state specific proximity and inhibition as closed-state specific proximity, two mutually exclusive possibilities.

There are two general ways in which both potentiation and inhibition could be observed. Both potentiation and inhibition could be present in every channel, with each channel behaving in the same way. Alternatively, Cu/P could produce two populations of channels, each showing only potentiation or only inhibition.

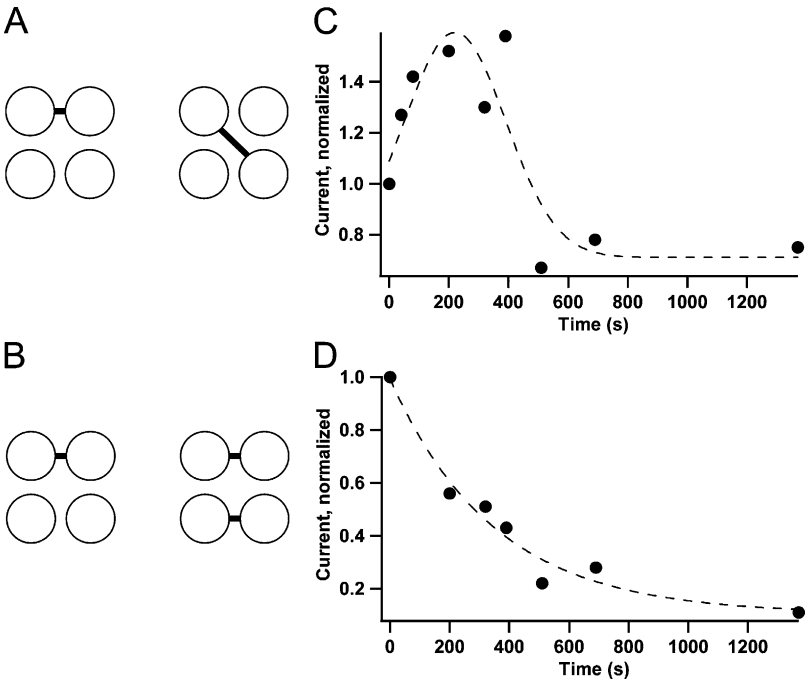

FIGURE 6. Mechanisms of the dual effects of Cu/P on 418C. (A) Disulfide bonds formed between opposite and adjacent subunits could produce different effects. (B) The number of disulfide bonds could determine whether potentiation or inhibition would be observed. (C and D) Kinetics of the Cu/P effect on 418C with currents activated by either (C) 2 μM cGMP or (D) 2 mM cGMP. The smooth curves represent Gaussian fits (C) and exponential fits (D).

One simple way for each channel to show both inhibition and potentiation is if an intersubunit disulfide bond between 418C subunits causes a decrease in channel conductance (the decrease in the maximal current), but an increase in channel open probability (the potentiation at subsaturating cGMP). The proximal C-linker region is at the end of S6, a likely location of the channel gate (Flynn and Zagotta, 2003). It is conceivable that a conformational change in this region induced by disulfide bond formation could cause changes in both ion permeation and in gating. The second general way to produce potentiation and inhibition is if two populations of channels are present, one with a decreased open probability, and the other with an increased open probability. We ought to be able to distinguish between these two models using single-channel recording.

We recorded the activity of single 418C and $CNGA1_{cysless}$ (as a control) channels before and after treatment with Cu/P (Fig. 5, left), and plotted all-points histograms to determine their open probability (Fig. 5, right). In each experiment, Cu/P was applied for 10 min, and currents were recorded at +50 mV with a low cGMP concentration (as indicated in the figure legend). The single channel conductance was 26 pS for both channels before Cu/P application, which was in the same range as that of the wild-type CNGA1 channel (Sunderman and Zagotta, 1999). Interestingly, we found that Cu/P treatment produced two populations of channels in 418C, one potentiated and the other inhibited. Among the seven patches tested, three of them showed an increase in open probability (P_o) at 4 μM cGMP after Cu/P application (Fig. 5 A, P_o = 0.09 ± 0.012 initially, P_o=0.83 ± 0.087 after Cu/P). For a saturating concentration of cGMP (2 mM), the P_o in these patches was initially 0.91 ± 0.054 and was 0.90 ± 0.066 after Cu/P treatment (unpublished data). The single channel conductance was not altered by Cu/P treatment. This indicates Cu/P potentiated 418C through an effect on channel gating. For the other four patches, P_o was 0.08 ±0.001 initially, and was reduced to essentially zero after Cu/P treatment both at 4 μM (Fig. 5 B) and 2 mM cGMP (not depicted). In all four of these inhibited patches, we recorded a total of <10 opening events after Cu/P treatment. This rate of opening was not sufficient to calculate P_o, but is interesting because those few openings that were observed had the same unitary conductance as observed before Cu/P treatment (unpublished data). The inhibition of this population of channels correlates with the inhibition of current produced by Cu/P treatment at the macroscopic level. As a control, we also measured the single-channel effects of Cu/P treatment on $CNGA1_{cysless}$ channels. We did not find a significant effect of Cu/P on the open probability or the single-channel conductance (Fig. 5 C; at 2 μM cGMP, P_o = 0.03 ± 0.014 initially, P_o = 0.09 ± 0.026 after Cu/P, n = 2, single channel conductance = 26 pS).

There are at least two ways in which Cu/P could produce two populations of channels. One is if a disulfide bond formed between opposite subunits produced one effect (e.g., potentiation), but disulfide bond formation between adjacent subunits produced another effect (e.g., inhibition; Fig. 6 A). Another possibility is

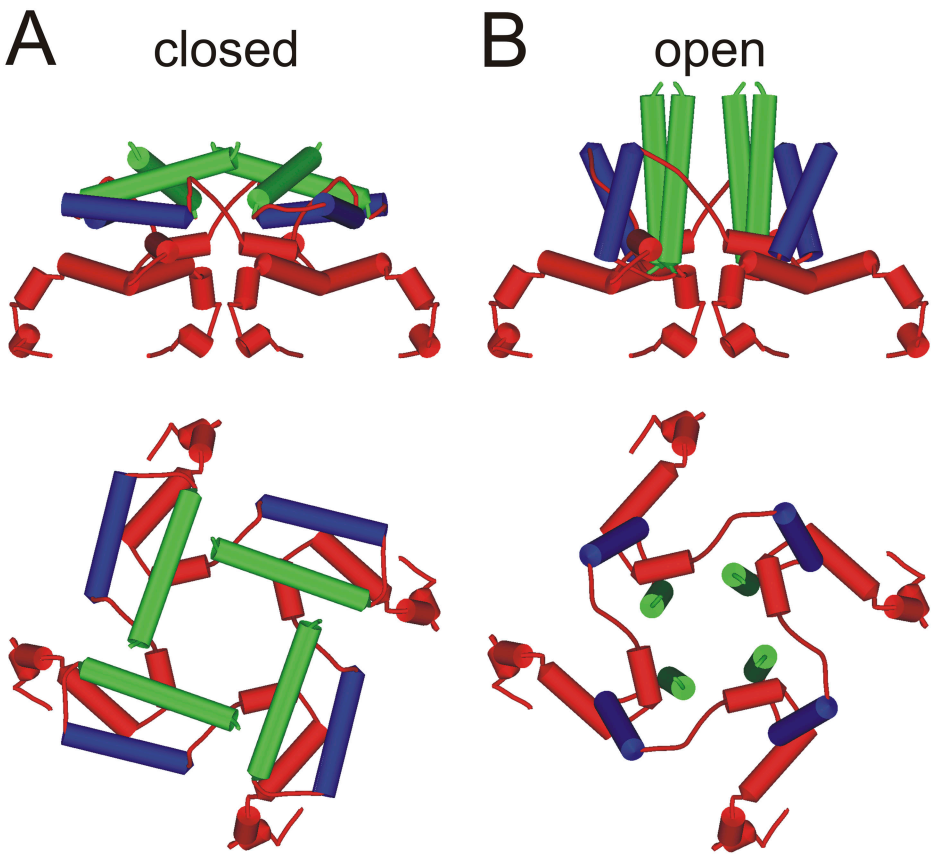

FIGURE 7. Cartoon model of closed and open channels. Side (top) and top (bottom) views of the CNGA1 C-linker made from the HCN2 structure (A) and from a model based on our data (B). The A' helices are shown in green and the B' helices are shown in blue. A and B differ only by the conformation of the B'-C' loop.

that the number of disulfide bonds per channel is important. With four subunits each containing one cysteine, it is possible that one disulfide bond might form, resulting in potentiation, but that later a second forms, resulting in inhibition (Fig. 6 B). To address this question, we examined the time dependence of the effects of Cu/P on 418C (Fig. 6, right). In the model shown in Fig. 6 B, it might be expected that one effect (e.g., potentiation) might be observed early, with formation of one disulfide bond, followed later by the second effect (e.g., inhibition) when the second disulfide bond formed. We measured the current after various times exposed to Cu/P, and plotted it versus cumulative Cu/P treatment time at subsaturating and saturating cGMP concentrations (Fig. 6, C and D). We found that Cu/P produced an initial increase in current activated by 2 μM cGMP, followed by a decrease in the current. In contrast, Cu/P produced only a slow decrease in the current activated by 2 mM cGMP, where the P_o initially was already near 1. This experiment suggests that the two populations of channels we observed in the single channel studies reflected channels with either one (potentiated) or two (inhibited) disulfide bonds present per channel. The distribution of potentiated versus inhibited channels observed would depend on the arbitrary time chosen for the Cu/P treatment. Thus, the potentiation we observed in Figs. 2 and 3 indeed represents open-state specific proximity, but is complicated at later times by a formation of a second disulfide bond, giving channel inhibition.

DISCUSSION

Is the crystal structure of the HCN2 C-linker a reasonable model for that of CNG channels? The sequences of HCN2 and CNGA1 in this region are 22% identical and 45% conserved (Fig. 1 A), suggesting that they likely have a similar structure. Equally important, they perform similar roles in the two channel types. We and others have shown that the C-linker of CNG channels energetically couples cyclic nucleotide binding to opening of the pore (Gordon and Zagotta, 1995a,b; Tibbs et al., 1997). In HCN channels, it has been shown that the C-linker inhibits opening of the pore, and that this inhibition can be relieved by cAMP binding to the CNBD, by deleting the C-linker and CNBD, or by deleting the CNBD (Wainger et al., 2001). Thus, the C-linker regions of the two channel types share sequence similarity and are functionally homologous; it seems likely that they are structurally homologous as well.

In the homology model of the C-linker of CNGA1 shown in Fig. 1 B, the residues at the 420 position of both adjacent and opposite subunits are much too far apart to either form a Ni^{2+} coordination site (420H) or

to form a disulfide bond (420C). Our data now show that the functional proximity between subunits is observed not only at the 420 position, but at 417 and 418 as well. Furthermore, in all cases, formation of a disulfide bond between cysteines at a given site produced potentiation. Potentiation of gating indicates an energetic stabilization of the open conformation of the channel relative to the closed conformation. Another way to state this is that the channels require less energy to open when the disulfide bond is formed compared with when the cysteines are reduced and the A' helices are free to move. We infer from this potentiation that the conformation of the channel trapped by the disulfide bond most closely resembles the open conformation.

Our data are incompatible with a model in which 417, 418, and 420 in different subunits are tens of Angstroms apart, as depicted in Fig. 1 B. We are led, then, to propose the following model for intersubunit interactions in the C-linkers of both CNG and HCN channels. Our hypothesis is depicted in Fig. 7. This cartoon shows the C-linker region represented in both the closed and open state. The closed state (Fig. 7 A) is identical to that of the HCN2 crystal structure. Although cAMP is bound to the CNBD in the HCN2 crystal structure, and the CNBD structure likely represents that of the open configuration, we believe that the C-linker in the structure is in the closed conformation. For the open state (Fig. 7 B), we have rotated the A' and B' helices as a unit, by introducing a rotation around the B'-C' loop. This rotation brings the A' helices nearly perpendicular to the membrane, as in the Johnson and Zagotta model (Johnson and Zagotta, 2001). We moved both the A' and B' helices as a unit because movement around the A'-B' loop alone could not bring the 417–420 positions close enough to form a disulfide bond. However, the required proximity between the A' helices does not uniquely constrain the B' helices or other regions of the model. In functional channels, binding of cyclic nucleotide to the CNBD (not depicted) would cause a conformational change from the closed state, with A' helices at a distance, to the open state, with A' helices in proximity. This conformational change would be directly coupled to opening of the ion-conducting pore.

Why does locking subunits together through disulfide bond formation potentiate gating, but not lock the channels open? A given energetic stabilization of the open state relative to the closed state could produce either a locked open channel or a potentiated channel, depending on the relative stability of the two states in the absence of disulfide bonds. Furthermore, formation of a disulfide bond between two subunits traps them only along one axis of symmetry. The two pairs of subunits are still free to move relative to each other; perhaps this movement facilitates closing. Finally, the disulfide bonds formed here trap the subunits at only one point. It is likely that the opening conformational change involves a concerted movement throughout all the subunits. Restricting the movement of the protein at just one point does not appear to be sufficient to prevent closing. Of course, we must exercise caution when drawing conclusions about the structure of the channel in the absence of disulfide bonds from the perturbed structure when disulfide bonds are present. Closed channels whose subunits are locked together by disulfide bonds are very likely to have a different structure than closed channels without disulfide bonds, at least in the arrangement of the A' helices.

What is the source of the two types of intersubunit interactions observed in 418C? Could one population arise from disulfide bond formation between subunits of different channels? Our observation of two populations at the single-channel level indicates this is not the case. We present two different ways different populations could arise in Fig. 6. In one model, disulfide bonds could form between either adjacent or opposite subunits, each with a different functional effect (Fig. 6 A). In the second model, formation of one disulfide bond would produce one effect, and formation of the second would produce the opposite functional effect (Fig. 6 B). We observed that the current activated by 2 μM cGMP was first potentiated by Cu/P, and was then inhibited after longer cumulative exposure to Cu/P. Although this time dependence does not rule out the model in which the two functional populations are based on disulfide bonds with two different orientations, it would seem that time dependence is more compatible with the model in which the two functional populations are based on having either one or two disulfide bonds. The potentiated population, observed with short time Cu/P treatments, would arise from formation of a single disulfide bond. The inhibited population would then arise later, as the second disulfide bond formed.

Inhibition of CNGA2 channels with Ni^{2+} has also been reported (Gordon and Zagotta, 1995b). Wild-type CNGA2 channels have a histidine at the position corresponding to 417, and a glutamine at the position corresponding to 420. Treatment of wild-type CNGA2 channels with Ni^{2+} shifts the dose–response relation for cGMP to the right, increasing the $K_{1/2}$ from 2.3 to 6 μM (Gordon and Zagotta, 1995b). The inhibition of CNGA2 channels by Ni^{2+} is unambiguous. We propose that this inhibition arises from the same mechanism that produced inhibition in CNGA1-417H. However, subtle differences in structure between CNGA1 and CNGA2 might prevent the relatively small potentiation produced by Ni^{2+} in CNGA1-417H from occurring in CNGA2. This is most likely to occur if 417 is at a posi-

tion that undergoes less movement during channel gating, relative to 420. Our model in Fig. 7 depicts 417 as near the fulcrum for movement, with proximity between subunits in both open and closed channels.

In summary, we have used trapping of the A' helices through disulfide bond formation to ask whether the crystal structure of the C-linker of HCN2 represents an open or closed conformation in CNG channel. Because each subunit contains only a single cysteine, any disulfide bond formation must occur between the same cysteine on different subunits. Three positions, 417, 418, and 420, formed disulfide bonds that potentiated activation of the channels. We interpret this potentiation to mean that the disulfide bond trapped the channels in a conformation more similar to the open state than to the closed state. These data are not compatible with a model in which the C-linker of the HCN2 structure represents the open channel conformation. Although cAMP is bound to the CNBD in the crystal structure and the CNBD observed in the structure almost certainly represents the open-channel conformation, our results indicate that the C-linker may be in the closed-channel conformation. Furthermore, the open-state specific proximity between subunits in the 417–420 region indicates that the A' helices form tilted bundles perpendicular to the axis of the membrane in open channels. Channel closure may then involve a relaxation of the A' helices to the position parallel to the axis of the membrane, as observed in the crystal structure of HCN2.

We are grateful to Dr. William N. Zagotta (University of Washington) for supplying the CNGA1 wild type and $CNGA1_{cysless}$ constructs. We thank Drs. Carmen A. Ufret-Vincenty, J.P. Johnson Jr., Noah Shuart, and Tamara Rosenbaum for reading an early version of the manuscript, Dr. Kerry Kim for helping with Igor programming, and Noah Shuart for making several of the constructs used here.

This work was funded by a generous grant from the National Eye Institute (R01 EY013007 to S.E. Gordon).

David C. Gadsby served as editor.

Submitted: 28 September 2004
Accepted: 24 January 2005

REFERENCES

Falke, J.J., A.F. Dernburg, D.A. Sternberg, N. Zalkin, D.L. Milligan, and D.E. Koshland Jr. 1988. Structure of a bacterial sensory receptor. A site-directed sulfhydryl study. *J. Biol. Chem.* 263:14850–14858.

Flynn, G.E., and W.N. Zagotta. 2003. A cysteine scan of the inner vestibule of cyclic nucleotide-gated channels reveals architecture and rearrangement of the pore. *J. Gen. Physiol.* 121:563–582.

Gordon, S.E., D.L. Brautigan, and A.L. Zimmerman. 1992. Protein phosphatases modulate the apparent agonist affinity of the light-regulated ion channel in retinal rods. *Neuron.* 9:739–748.

Gordon, S.E., and W.N. Zagotta. 1995a. A histidine residue associated with the gate of the cyclic nucleotide-activated channels in rod photoreceptors. *Neuron.* 14:177–183.

Gordon, S.E., and W.N. Zagotta. 1995b. Localization of regions affecting an allosteric transition in cyclic nucleotide-activated channels. *Neuron.* 14:857–864.

Gordon, S.E., and W.N. Zagotta. 1995c. Subunit interactions in coordination of Ni^{2+} in cyclic nucleotide-gated channels. *Proc. Natl. Acad. Sci. USA.* 92:10222–10226.

Guex, N., and M.C. Peitsch. 1997. SWISS-MODEL and the Swiss-PdbViewer: an environment for comparative protein modeling. *Electrophoresis.* 18:2714–2723.

Jan, L.Y., and Y.N. Jan. 1990. A superfamily of ion channels. *Nature.* 345:672.

Jan, L.Y., and Y.N. Jan. 1992. Tracing the roots of ion channels. *Cell.* 69:715–718.

Johnson, J.P., Jr., and W.N. Zagotta. 2001. Rotational movement during cyclic nucleotide-gated channel opening. *Nature.* 412: 917–921.

Kaupp, U.B., T. Niidome, T. Tanabe, S. Terada, W. Bonigk, W. Stuhmer, N.J. Cook, K. Kangawa, H. Matsuo, T. Hirose, et al. 1989. Primary structure and functional expression from complementary DNA of the rod photoreceptor cyclic GMP-gated channel. *Nature.* 342:762–766.

Kaupp, U.B., and R. Seifert. 2002. Cyclic nucleotide-gated ion channels. *Physiol. Rev.* 82:769–824.

Kobashi, K. 1968. Catalytic oxidation of sulfhydryl groups by o-phenanthroline copper complex. *Biochim. Biophys. Acta.* 158:239–245.

Maroney, M.J. 1999. Structure/function relationships in nickel metallobiochemistry. *Curr. Opin. Chem. Biol.* 3:188–199.

Matulef, K., G.E. Flynn, and W.N. Zagotta. 1999. Cysteine-scanning mutagenesis of the cyclic nucleotide-gated channel ligand binding domain. *Biophys. J.* 76:A337.

Molokanova, E., B. Trivedi, A. Savchenko, and R.H. Kramer. 1997. Modulation of rod photoreceptor cyclic nucleotide-gated channels by tyrosine phosphorylation. *J. Neurosci.* 17:9068–9076.

Paoletti, P., E.C. Young, and S.A. Siegelbaum. 1999. C-linker of cyclic nucleotide-gated channels controls coupling of ligand binding to channel gating. *J. Gen. Physiol.* 113:17–34.

Richards, M.J., and S.E. Gordon. 2000. Cooperativity and cooperation in cyclic nucleotide-gated ion channels. *Biochemistry.* 39: 14003–14011.

Rosenbaum, T., A. Gordon-Shaag, M. Munari, and S.E. Gordon. 2004. Ca^{2+}/calmodulin modulates TRPV1 activation by capsaicin. *J. Gen. Physiol.* 123:53–62.

Sunderman, E.R., and W.N. Zagotta. 1999. Sequence of events underlying the allosteric transition of rod cyclic nucleotide-gated channels. *J. Gen. Physiol.* 113:621–640.

Tibbs, G.R., E.H. Goulding, and S.A. Siegelbaum. 1997. Allosteric activation and tuning of ligand efficacy in cyclic-nucleotide-gated channels. *Nature.* 386:612–615.

Torchinskii, I.U. 1974. Sulfhydryl and Disulfide Groups of Proteins. Consultants Bureau, New York. 275 pp.

Wainger, B.J., M. DeGennaro, B. Santoro, S.A. Siegelbaum, and G.R. Tibbs. 2001. Molecular mechanism of cAMP modulation of HCN pacemaker channels. *Nature.* 411:805–810.

Zagotta, W.N., N.B. Olivier, K.D. Black, E.C. Young, R. Olson, and E. Gouaux. 2003. Structural basis for modulation and agonist specificity of HCN pacemaker channels. *Nature.* 425:200–205.